Smart Transformer/Large Flexible Transformer

Rongwu Zhu, *Member, IEEE*, Markus Andresen, *Member, IEEE*, Marius Langwasser, *Student Member, IEEE*, Marco Liserre, *Fellow, IEEE*, Joao Pecas Lopes, *Fellow, IEEE*, Carlos Moreira, Justino Rodrigues, and Mario Couto

***Abstract*—Solid-state transformer-based smart transformer (ST) can provide the dc connectivity and advanced services to improve the grid performance and to increase the penetration of the power electronics interfaced resources (e.g., distributed generators and electric vehicle charging stations) in modern electricity distribution grids. Since the ST is a new and effective paradigm of the electricity grid evolution to well understand the ST, this paper systematically presents the basic architecture and the typical control schemes of the ST and then the advanced services that ST can provide to improve the electricity grids performances in terms of the power flow control, power quality improvement, active damping and active contribution to improve distribution grid resilience by means of enabling autonomous microgrids operation as well as launching a restoration procedure following a general blackout.**

***Index Terms*—Smart Transformer, voltage control, power quality, active distribution grid black start.**

I. Introduction

The development of low carbon technologies (e.g., generation and utilization of renewables), challenges the modern electricity grids performances in terms of the stability, power quality and reliability[1], [2]. Thus, the update of grid assets, advanced monitoring and control techniques are needed to improve the electricity grid performances, and to further increase the penetration of renewables [3]–[5].

The solid-state-transformer-based smart transformer (ST) was proposed to effectively solve the aforementioned challenges caused by high penetration of renewables in the distribution electricity grids, due to the advanced control functions and the provision of dc connectivity as well [3]. Moreover, the ST represents a new semi-centralized scheme to avoid extreme decentralization caused by the high penetration of power electronics-interfaced (PEI) distributed energy resources (DERs).

The design of the hardware architecture (e.g. topology, building blocks, component sizing) of the ST is determined by the services that the ST should provide to the grid [6].The three-stage configuration of the ST offers dc connectivity, which makes the ST an active, multi-port node, allowing for e.g., storage integration [7] and meshed, hybrid grid operation [8]. The meshed reconfiguration of the grid can help to increase the renewable energy sources (RES) share, while keeping the grid expansion effort low and the quality of power supply high.

In order to operate the ST in a proper way, the ST is controlled either in grid-forming (GFM) or in grid-following (GFL) mode, according to the network structure and the required grid supports. In comparison, besides the different synchronization mechanism, the GFM operation of ST emulates the synchronous machine behavior while the GFL operation is suitable for high current quality applications.

In grid applications, the ST can effectively control the power flow in either the radial networks or meshed and hybrid networks, where the optimal power flow control can avoid high voltage violation, high line losses and overload of grid assets. Based on the included power conversion stages, the ST can also provide a full decoupling of the medium voltage (MV) and low voltage (LV) side grids frequencies. Such frequency decoupling can have an important role regarding the possibility of exploiting power-frequency droop-based controllers in LV-connected generators or specific loads (as for example electric vehicle (EV)-chargers) in order to locally promote some form of generation-load balancing [9]. Moreover, some coordination strategies between the LV and MV side frequency can be envision alongside a ST in order to allow LV-connected resources to actively respond to frequency events occurring in the upstream grid [9].

One of the new characteristics caused by high penetration of PEI resources in the electricity grids is the harmonic interaction, which degrades the power quality (voltage and current) of the electricity grids [1], arises resonant issues and reduces stability margin [10]. The output impedance of ST may be higher than the conventional power transformer (CPT), because the switching characteristics of the power converter in ST requires an output filter to suppress the switching harmonics. The higher output impedance is the main reason to cause the power quality issues [11]. The resonant and stability issues are caused by both the impedance gain and phase characteristics of the interconnected systems, according to the impedance-based stability criterion. These issues can be solved by improving the control schemes of the interfaced power converters of DERs, but such solution results in the customized function of the DERs potentially increasing the cost and moreover the effectiveness is degraded in case of the change of grid operating conditions caused by the continuous increase penetration of DERs. Thus, the effective control solutions implemented inside the ST instead of the DERs to improve the power quality [11] and to stabilize [10] the grid will be presented in this paper.

Manuscript received August 11, 2020; Revised October 22, 2020; Accepted November 19, 2020. Date of publication December 25, 2020; Date of current version December 18, 2020.

The authors gratefully acknowledge funding by the German Federal Ministry of Education and Research (BMBF) within the Kopernikus Project ENSURE "New ENergy grid StructURes for the German Energiewende" (03SFK1I0-2) (*Corresponding author Rongwu Zhu*)

R. Zhu, M. Andresen, M. Langwasser, M. Liserre are with Chair of Power Electronics, Kiel University, Germany (rzh, ma, mlan, ml@tf.uni-kiel.de)

J. Pecas Lopes, C. Moreira, J. Rodrigues and M. Couto are with (jpl@fe.up.pt, carlos.moreira@inesctec.pt, justino.m.f.rodrigues@gmail.com, mario.teixeira.couto@gmail.com)

Digital Object Identifier 10.30941/CESTEMS.2020.00033

Aiming to contribute to increase the resilience of active distribution grids, the ST can be envisioned as a key enabler of the autonomous operation mode of MV and LV distribution grid sections under a multi-micro-grid concept following catastrophic events occurring upstream. The dc connectivity provided to integrate a local energy storage system (ESS), together with the flexibility to operate its power conversion stages in GFM or GFL modes is fundamental in order to enable autonomous operation mode of a multi-microgrid through a (fleet of) ST. Moreover, the ESS envisioned to exist in future active distribution grids together with locally available DERs allows to properly coordinate a service restoration stage at the MV and LV level in case a general blackout occurs. Both operation modes are key contributions within the scope of increasing distribution grid resilience.

The rest of this paper is organized as follows. The voltage and current source inverter-based architectures and their possibility to enable an active node for ac, dc and hybrid grid operation in radial and meshed network are briefly introduced in Section II. The control mode of ST in GFL and GFM operation, which allows the ST to be equivalent to a slack bus, *P* and *Q* bus, is studied in Section III. The ST provided advanced services in terms of power flow control, power quality improvement, active damping, frequency support and black start functions are studied in Section IV. Section V concludes this paper.

II. General Architecture

A. Hardware Solutions

Several authors proposed topologies for STs and several reviews grouped them by certain characteristics, like power conversion stages or the adopted converter architecture [12],[13]. The installation of the ST in the electricity grid is motivated by the services it can provide. Therefore, the hardware needs to be designed in such a way that it meets the requirements of the grid operator as well as the grid conditions. These parameters are commonly power system related and may be related to parameters such as:

- •DC-connectivity and DC voltage range
- •Efficiency
- •Power quality
- •Voltage range of the connected ac grids
- •P/Q characteristics
- •Grid synchronization dynamics
- •Maximum space
- •etc.

Several of these parameters are linked to the design of the system and compliance with certain requirements may be easier for certain topologies than for others. Therefore, the requirements need to be translated into the design of the ST hardware. This covers the following aspects:

- •Topology choice
- •System modularity including the number of building blocks
- •Component sizing
- •Control system
- •Grid synchronization algorithm
- •etc.

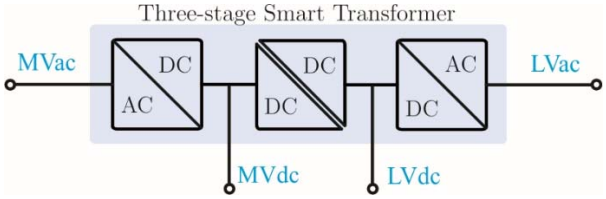

Fig. 1. Three-stage ST topology.

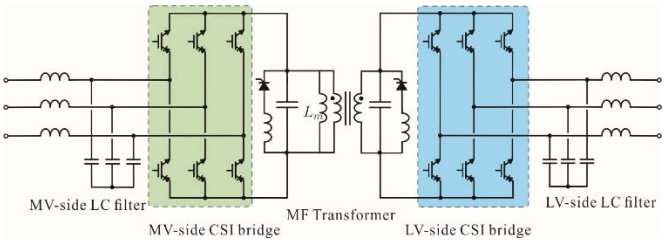

Fig. 2. ST topology of the S4T.

As a practical example, a transformer substation shall be replaced by an ST, which shall providedc-connectivity and needs to fit the space where the substation was installed before. Consequently, a medium frequency transformer is needed due to the space requirements and the dc-connectivity, which excludes several possible ST architectures. Nevertheless, there is still a large range of possibilities: As an example, a three-stage ST is shown in Fig. 1, which is commonly referred to be most flexible for providing services. This topology has two dc connections for connecting ESSs or possibly dc-grids. This enables direct control of the grid voltage profile [7].

Moreover, the topology affects the required volume of the system by means of the selected modularity and the frequency of the isolation stage. For the three-stage ST topology the most common use case is the operation of the LV side converter in GFM, the isolation stage in LVdc control and the MV side in GFL.

The component sizing determines the power transfer capability of the grid and therefore a possible margin for a future load increase, overload capability and the maximum output voltage for controlling transients. As it has been presented in [6], the sizing even impacts the potential for providing services. For ensuring low losses during operation, the target efficiency shall also be determined. In addition power quality related measures like the Total Harmonic Distortion (THD) of the output voltage (in GFM operation) or the output current (in GFL operation) shall be defined. This point will be examined in Section III A. Remarkably, the output voltage range is another important measure to provide the demanded voltage control range, which may be required to ride through faults without disconnecting the grid.

Examples for ST topologies are examined in [3], where the topologies have been grouped by the number of power conversion stages. Moreover, the modularity is discussed and solutions range from monolithic solutions to modular solutions with a high number of building blocks. As an example for a single stage ST, the S4T topology is shown in Fig. 2. The S4T is a current source based converter topology [14], which has significant less components in comparison to commonly

proposed modular voltage source converter topologies. Remarkable differences are the simple fault handling capability of the S4T, because of the current source topology with few bidirectional power semiconductors in contrast to the high number of building blocks and transformers.

B. An Active Node Connecting AC to DC Grids

The ST enables to interconnect multiple ac and dc grids. As inherently stated in a commonly used description of the ST, Energy Router, a key functionality is the energy flow control. This means, the ST can in contrast to a CPT-control the active and the reactive power exchange with the connected grids. This enables to obtain an intelligent node, scaling up to a system with multiple intelligent nodes in the grid.

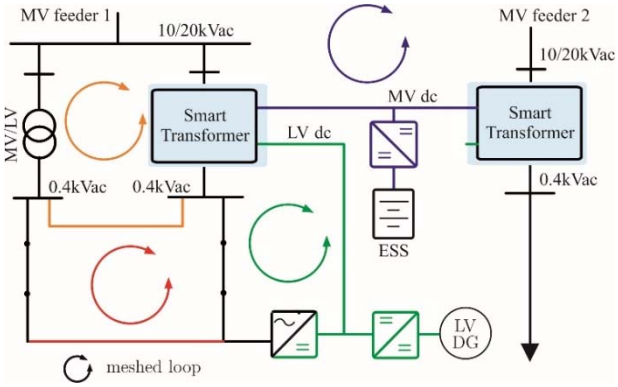

Fig. 3 ST-enabled configurations of a meshed hybrid distribution grid.

Two architectures are commonly used to build the MV side ac/dc converter of the ST. The MMC-based architecture, which in contrast to the CHB one, is a truly multiport architecture and offers an additional MV dc port. However, this comes at the costs of an increased number of cells and semiconductor devices.

In the configuration to interconnect ac and dc grids, commonly meshed grids are obtained, which provide high potential for reduced grid reinforcements or operation with reduced losses. However, the control and the protection remain challenging [8]. In general, a meshed grid refers to a system, in which each grid node is supplied from at least two sides, allowing for advanced power flow control by means of the ST. As shown in Fig. 3 the ST enables the meshed hybrid distribution grid in four different configurations. The first option (shown in orange) is to connect two parallel feeders(e.g. one ST-fed and one fed by CPT) at the low voltage ac busbar. This allows for equal distribution of the load power demand among the feeders and significantly improves the appliances overload condition and feeder voltage profile [8]. Similar benefits can be obtained, if the grid is reconfigured to a ring grid by closing the normally open point (NOP) at the end of the LV feeders (shown in red in Fig. 3).

The growing amount of DERs and ESS units increases the number of power conversion stages in the grid. The use of multiport ST facilitates the integration of these devices and can help to keep the grid infrastructure light, providing advanced services in both ac and dc grids. In [15], the use of an extra LVdc line is proposed, which interconnects the ST LVdc link with the dc bus of distributed generation converters and dc loads (highlighted in green in Fig. 3). Several active power flow paths are made available through this architecture, such that the active power supply is near to the load points and is drawn from ST, only in times where the DERs are absent. This reduces the size of the ST's LV ac/dc converter, improves the utilization of DERs converter and ensures reverse power flow at higher efficiency. In [16], a novel interconnected design of a multiport ST is proposed to further increase the efficiency in the meshed hybrid ac and dc grid.

As fourth option, in a scenario with two distinct MV grid with different supply structure, i.e. one DG-dominated and one load-dominated, the MVdc links of two ST can be coupled via an additional MVdc line (in blue in Fig. 3). This improves the supply redundancy and provides the possibility to fulfill the power demand of the two MV feeders by a single storage unit in case of grid fault emergency.

III. CONTROL OF ST

According to the control scheme and corresponding physical mechanism, the operation of ST can be defined as GFL and GFM mode, with the equivalent physical models as shown in Fig. 4.

A. Control of ST in GFL Operation

In the GFL mode, the ST is controlled as a current source to inject a controllable current into the electricity grid. The phase angle information of grid voltage at the connected point of the ST is needed in order to decouple the active and reactive component of the injected current accurately, and various phase-locked-loop (PLL) techniques were proposed in literature to detect the grid voltage phase information, as shown in Fig. 4(a).

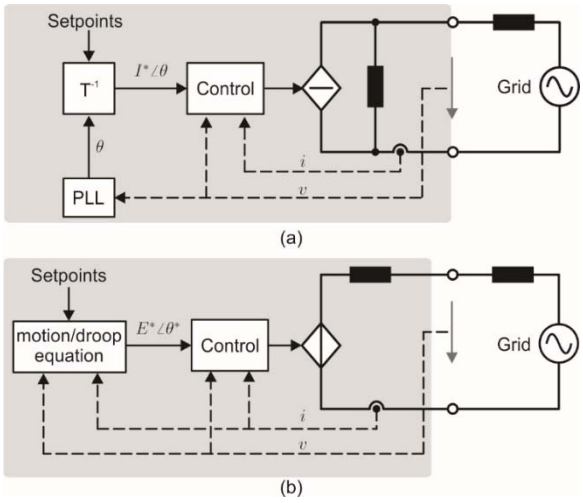

Fig. 4. Equivalent circuit of the ST operating in (a) GFL and (b) GFM.

The detailed control block diagram of ST operating in GFL mode is shown in Fig. 5, where G_i is the current controller, G_{Lf} is the transfer function of the ac filter inductor, G_{Cf} is the transfer function of the ac filter capacitor, G_d is the transfer function of delay.

The current reference, i^*, can be computed by the active and

reactive power reference, p^* and q^*, directly,

$$i^* = \begin{vmatrix} i_d^* & i_q^* \end{vmatrix}' = C_{p,q} \begin{vmatrix} p^* & q^* \end{vmatrix}' \tag{1}$$

where $C_{p,q} = \frac{2}{3u_d}\begin{vmatrix} 1 & 0 \\ 0 & -1 \end{vmatrix}$, subscripts "d" and "q" represent the d- and q-axis component in the synchronization reference frame.

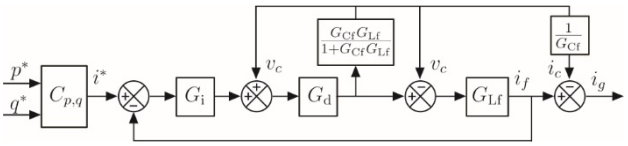

Fig. 5. Control block diagram of GFL operation.

B. Control of ST in GFM operation

In the GFM mode, the ST is controlled as a voltage source, as shown in Fig. 4(b). The active and reactive power are controlled by adjusting output voltage amplitude and phase angle of the ST, with respect to power synchronization mechanism, when the line is more inductive. Based on the two sources model as shown in Fig. 6, the active and reactive power flow at the receiving end can be obtained as:

$$\begin{aligned} p &= \frac{U\left(E\cos\delta - U\right)\cos\beta + EU\sin\delta\sin\beta}{z} \\ q &= \frac{EU\sin\delta\cos\beta - U\left(E\cos\delta - U\right)\sin\beta}{z} \end{aligned} \tag{2}$$

where p and q are the active and reactive power, respectively, E and δ are the amplitude and angle of voltage at the sending end, U is the voltage amplitude at the receiving end, z and β are the amplitude and angle of line impedance.

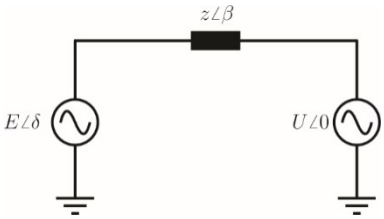

Fig. 6 Model of two-source system.

In (2), the active and reactive power are coupled with voltage amplitude and angle. Generally, they are approximately decoupled with respect to the x/r ratio of power line (q→f(δ) and p→v for resistive lines, and p→f(δ) and q→v for inductive lines). It is assumed that the line is inductive for the study in this paper.

The motion/droop characteristic of the GFM in Fig. 4(b) is derived by emulating the conventional synchronous generators. The swing equation of conventional synchronous generators is shown as,

$$p_{in} - p = J\frac{d\left(\omega - \omega_o\right)}{dt} + D\left(\omega - \omega_o\right) \tag{3}$$

where p_{in} is the input power, ω_o is the synchronous frequency, ω is the grid operating frequency, J is the inertia, D is the damping coefficient.

Due to the assumption of only inductive line, $\beta=\pi/2$, and linearizing (2) and (3) at the equilibrium points δ_o, ω_o and p_o, it can be obtained that,

$$\begin{aligned} \Delta p &= J\frac{d\Delta\omega}{dt} + D\Delta\omega \\ \Delta p &= \frac{EU\Delta\omega}{z} \end{aligned} \tag{4}$$

where Δ represents the increment. The reactive power in (2) can be further simplified as,

$$q = -\frac{UE - U^2}{z} \tag{5}$$

Similarly, when a voltage droop is used, the "q-v" characteristic is obtained as,

$$\Delta q = -\left(T_v\frac{d\Delta E}{dt} + \frac{U\Delta E}{z}\right) \tag{6}$$

where T_v is the time constant of voltage droop.

Based on (3), (4), (5) and (6), the control block diagram of the GFM inverter is shown in Fig. 7(a), in which G_{CU} is the closed-loop of voltage control as shown in Fig. 7(b), G_u is the voltage controller. In case ΔE=0 and $\Delta\delta$=0, the references of ST output voltage amplitude and angle are both fixed, and ST is operating as a slack bus (constant voltage and constant frequency). In case $\Delta E\neq0$ and $\Delta\delta\neq0$, as shown in Fig. 7(a), the ST is operating as a constant PQ bus.

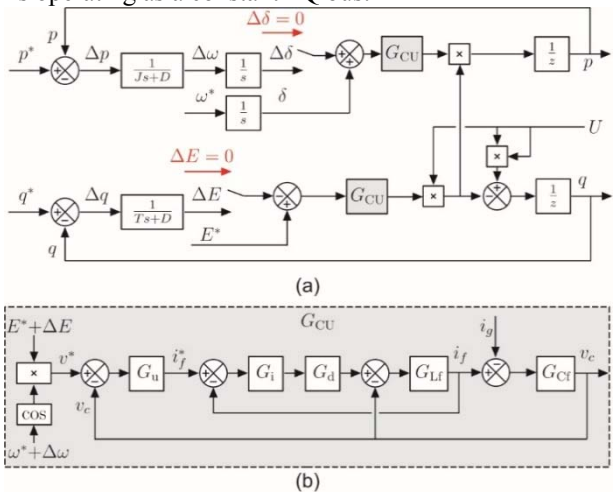

Fig. 7. Control block diagram of (a) overall system of GFM, and (b) voltage loop.

IV. IV. Advanced Services Provided By ST

A. Power Flow Controllability

1) Meshed LV networks: In the meshed LV ac grid operation, as shown in Fig. 8, the ST (T_1) and CPT (T_2) can operate either in equal power sharing control or in optimal power flow control [17]. The sensitivity coefficients for different bus voltages to active and reactive power variation are computed as,

$$\begin{aligned} k_{p,m} &= \frac{\partial v_m}{\partial p_{st}} \\ k_{p,m} &= \frac{\partial v_m}{\partial q_{st}} \end{aligned} \tag{7}$$

where m=L_1, L_2...L_{10}, representing the number of the critical bus

as shown in Fig. 8.

Based on (7), the minimum bus voltage variation control is obtained by the active and reactive power flow control in ST.

$$\min_{\Delta p_{st},\Delta q_{st}} \left\{ \sum_{m=1}^{10} \left(v_m + k_{p,m}\Delta p_{st} + k_{q,m}\Delta q_{st} - v^* \right)^2 \right\} \tag{8}$$

To simplify analysis, by assuming that the active power flow in the meshed LV ac grid is equally shared between the ST and CPT, i.e., p_{st}=p_{cpt}, as shown in Fig. 8(a), the minimum voltage variation optimization in (8) only involves the reactive power flow control and the simulation results under three different scenarios are compared in Fig. 8(b)-(d).

In case S2 is open, the high DG penetration leads to the bus voltages at L_4 and L_5 higher than 1.05pu, as shown in Fig. 8(b) and (d), while the high load demand results in the bus voltages at L_7, L_8, L_9 and L_{10} lower than 0.95pu, as shown in Fig. 8(b) and (c).

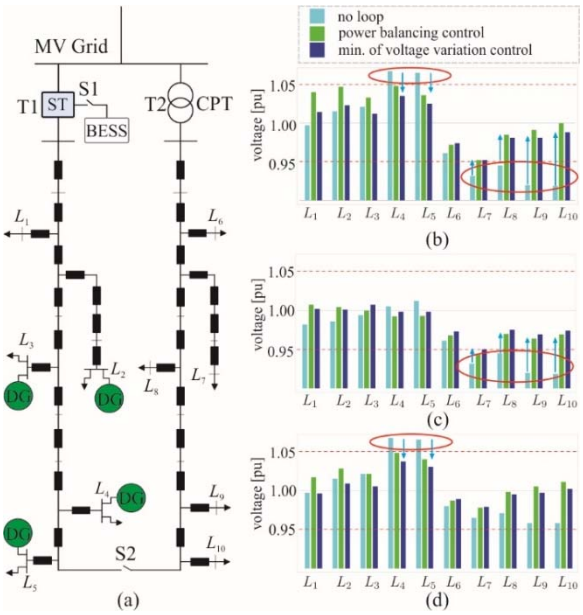

Fig. 8(a) structure of ST operating in meshed LV ac network, adapted from CIGRE LV benchmark mode, and voltage profile at different buses for different control schemes under (b) scenario 1: high DG penetration and high load demand, (c) scenario 2: low DG penetration and high load demand, and (d) scenario 3: high DG penetration and low load demand [17].

2) *Hybrid MV AC/DC networks*: Apart from the LV grids, the ST can also provide significant improvements in power flow controllability in hybrid MV ac/dc networks, and in both MV ac and dc sub-networks. Regarding reactive power flow controllability in MV ac networks, the ST's MV inverter provides great flexibility since it can be dispatched with total decoupling from the reactive power demand in ST's LV ac network [6]. Regarding active power flow controllability, the integration of ESS capacity in the ST enables the power dispatch of the ST's MV inverter, while meeting the power demand in ST's fed distribution networks [7].

However, the regulation of ST's MV dc bus voltage levels can also be exploited to control the active power flow in both MV ac and dc sub-networks. In order to exemplify the potentialities offered by ST in this subject, the hybrid MVac/dc network illustrated in Fig. 9 is considered here. In this example, only the modulation of the dc voltage in ST's MVdc bus is exploited to control the active power flow in the MV dc and ac sub-networks. In order to do so, a droop-based controller capable to adjust the dc voltage in ST's MV dc bus as a function of the active power exchanged by the ST's MVdc bus with the MV dc sub-network is incorporated V_{dc} (P_{dc}) droop, where droop slope and offset can be properly adjusted.

In the example illustrated in Fig. 9, the active power levels assigned to ST's LV networks and MV dc distributed resources originate a non-optimal active power flow in both ac and dc sub-networks if V_{dc}(P_{dc}) droops are not activated, as shown in the results presented in Fig. 10 - No Droop". By activating only the slope curve of V_{dc}(P_{dc}) droops (droops' offset is zero), significant improvements in active power flow can be obtained, as shown in Fig. 10 - "Slope on". This shows that active power flow in hybrid MV ac/dc networks can be improved by locally embedded automatic control mechanisms. However, further improvements can be obtained by combining the locally embedded automatic control mechanisms. In case of V_{dc}(P_{dc}) droops with additional control actions coming from higher-level control entities (e.g. System Operator), the regulation of the dc voltage offset parameter available in the V_{dc}(P_{dc}) droop controllers, as depicted in Fig. 10 - "OffsetOpt".

B. Power Quality Improvement and Active Damping

Unlike a CPT, the ST can not only isolate the harmonics at both the LV and MV ac grids, avoiding propagating from one side to another side, due to the existence of the dc-link, but also further improve the grid quality in terms of harmonics and resonance, due to the advanced control of the ST.

1) *MV ac grid current quality improvement:* Since the MVac/dc stage is always operating as an active front end and the ST is convenient to compensate the distorted current at the MV ac grid. Two cases are defined here (MV ac grid current is distorted defined as case 1, and MV grid current is distorted and unbalanced defined as case 2) to show the capability of ST to improve the MV ac current quality, as shown in Fig. 11(a). In case 1, with ST, the MVac current THD is reduced from 10.24% to 5.22%, and in case 2, the MVac current THD is reduced from 10.32% to 5.31%. In case2, for the CPT, the asymmetrical three-phase loads in LVac grid results in the unbalanced degree of MVac current is about 14.29%. In contrast, the ST can control the unbalanced degree of MVac current to almost 0%, as shown in Fig. 11(b) [18].

2) *LV ac grid voltage quality improvement*: The high penetration of power electronic interfaced sources (DERs, EV charging stations and other loads) results in the harmonic interaction among the power electronics and nonlinear loads, significantly degrading the LV ac grid voltage quality. Based on the Thevenin model of ST Fig. 12(a) and the Ohm' Law, the ST output voltage is polluted by the distorted load currents in case the output impedance of ST is not zero, as shown in (9). Apart from the voltage harmonic issue, the dynamic performance of grid voltage during load step change is also degraded.

$$v_{pcc} = v_o - i_g z_{st} \tag{9}$$

where v_{pcc} is the ST output voltage at PCC, $_{vo}$ is the Thevenin

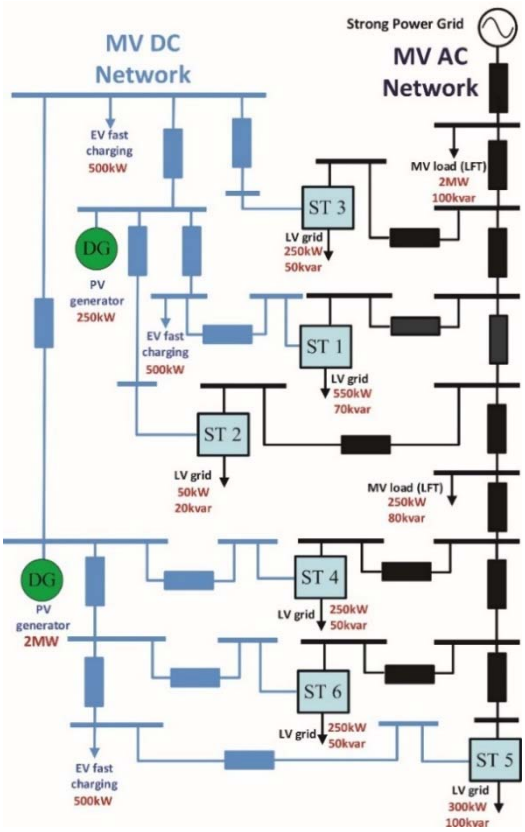

Fig. 9. Example of a hybrid MV network, with STs providing the interface between the ac MV network (black) and the dc MV network (blue).

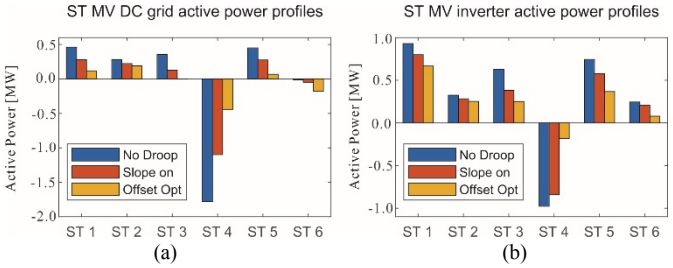

Fig. 10. Active power profiles in STs' MV dc and ac grid terminals, with nominal dc voltage in STs' MV dc-link (blue), with STs' MV dc-link voltage modulation using $V_{dc}(P_{dc})$ droop control (red) and with ST's MV dc-link voltage modulation using $V_{dc}(P_{dc})$ droop control plus V_{dc} offset control(yellow).

internal voltage of ST, z_{st} is the Thevenin output impedance of ST, i_g is the grid current.

Inspired by this law, the output impedance reshaping approach was proposed to improve the ST-fed LV ac grid voltage quality [19]. The experimental results of the ST-fed LV ac grid with diode loads and with and without DGs are compared in Fig. 13(a). In case of no DGs connection, the grid voltage is polluted by the diode load, and the THD is 10.85%, and the voltage THD is increased to 11.65% when the DGs is integrated due to the harmonic interaction between DGs and diode loads. In contrast, the LV ac grid voltage is improved to 4.52% with nonlinear loads, and 5.39% with DGs and nonlinear loads, respectively, when the power quality control is implemented in ST.

The dynamic performance of rapid voltage change during load step change is shown in Fig. 13(b). Without the output impedance reshaping approach, the depths of voltage sag and

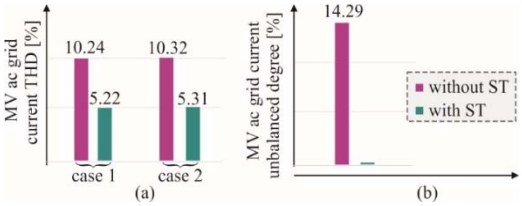

Fig. 11 Comparison of MV ac grid current (a) THD, (b) unbalanced degree[18].

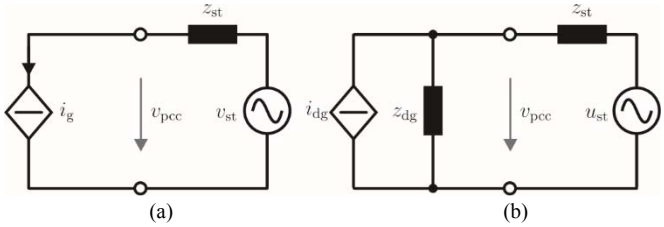

Fig. 12. Equivalent models, (a) Thevenin model of ST, (b) Thevenin mode of ST and Norton model of DG.

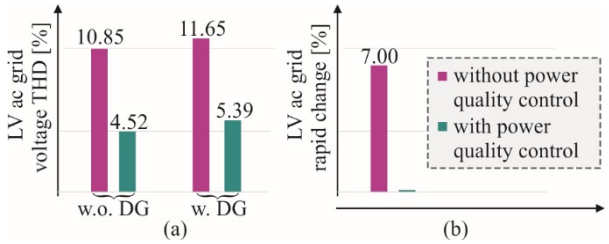

Fig. 13. Comparison of LV ac voltage quality, (a) with nonlinear diode loads and without and with DGs integration, (b) amplitude of rapid voltage change.

swell are both 7.00%, as shown in Fig. 13(b), while with the output impedance reshaping, the grid voltage is robust to load step change and the rapid change of voltage is almost 0.0% during the load step change, as shown in Fig. 13(b).

3) Resonance damping in LV ac grid: Based on theThevenin model of ST and Norton model of DG as shown in Fig. 12(b), the PCC voltage can been computed as,

$$v_{pcc} = \left(v_{st} + i_{dg} z_{st}\right) \frac{1}{1 + z_{st} / z_{dg}} \tag{10}$$

where z_{dg} and i_{dg} are the output impedance and injected current of the DG.

Based on z_{st}/z_{dg}, the bode diagram or Nyquist-based impedance stability criterion can be used to study the system stability of (10). Based on the impedance stability criterion, the low pass filter (LPF) and lead element filter (LEF) based active damping approaches were used to damp the resonance by reshaping either the ST output impedance amplitude or phase or both the output impedance amplitude and phase [10].The experimental results are shown in Fig. 14. When without the LPF-based active damping approach, the ST output voltage and DG injected current are distorted seriously as shown in Fig. 14(a), while the LFT-based active damping approach can stabilize the grid voltage and DG injected current, as shown in Fig. 14(b). Similarly, the performances of the LEF-based active damping approach are compared in Fig. 14(c) and (d).

C. Frequency Control in Islanding Operation Mode

The development of operation strategies for islanding mode requires the existence of ESS. Therefore, ST can play an important role to develop new control strategies for islanding operation, mainly, assuming that it is possible to connect ESS

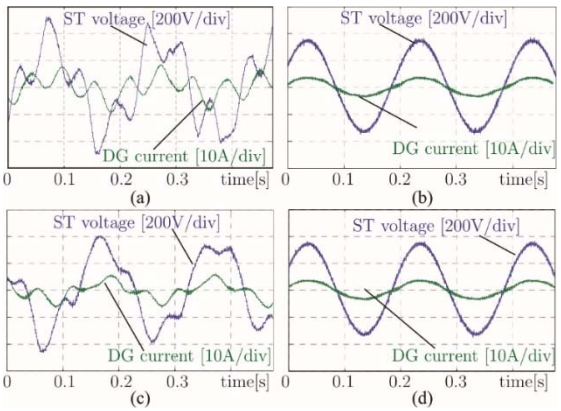

Fig. 14. Comparison of the system stability, (a) without and (b) with LPF-based active damping, (c) without and (d) with lead element filter (LEF)-based active damping active damping method [10].

in the dc-link. Following this approach, the ST leverages then the development of control strategies for islanding mode in Multi-Microgrids (MMG), by coordinating the operation of the ST power converters with the DERs connected to the grid. A MMG corresponds to a MV grid interconnecting several LV microgrids (MG) where distributed generators can be connected, as described in Fig. 15. At the LV level the MG integrates microgeneration units, local loads and energy storage systems. In the approach presented in [20], it is considered that in some secondary substations (SS), the traditional electromagnetic transformer is replaced by ST with a three-stage (ac/dc/ac) configuration. At the ST level, the MV and LV power converters will operate as a GFM unit or a GFL unit based on the existence of ESS in the dc-link. In this regard, with ESS connected to the dc-link, MV and LV grids can operate decoupled. Thus, the two grid interfaces correspond to GFM units creating voltage and frequency references for both sides.

When the dc-link does not have ESS, only the LV inverter is a GFM unit. This arrangement allows that the frequency at the LV side is decoupled from the MV grid. However, the MV inverter is operated as GFL unit, injecting or absorbing active power into/from the MV taking into consideration the load-generation balance within the MG. In what concerns there active power, there is a decoupling between the two sides of the ST.

1) Frequency Coordination Control at the ST level: For the second case described above (ST without ESS), the LV units connected to the LV grid will not be able to participate in the frequency control due the decoupling caused by the dc-link. Aiming to induce the participation of the LV DERs in the MV-side frequency control, a new droop-based control approach is proposed to modulate LV MG frequency as function of the MV frequency. Indeed, as LV ST inverter operates always as GFM, it is possible to change the ideal value of the angular frequency ω_o for the LV grid, as described in the following set of equations:

$$\omega_{oLV} = \begin{cases} \omega_{oi} + k_{fMV,} & f_{MV} > 50.2Hz \\ \omega_{oi,} & 50.2 \geq f_{MV} \geq 49.8Hz \\ \omega_{oi} - k_{fMV,} & f_{MV} < 49.8Hz \end{cases} \quad (11)$$

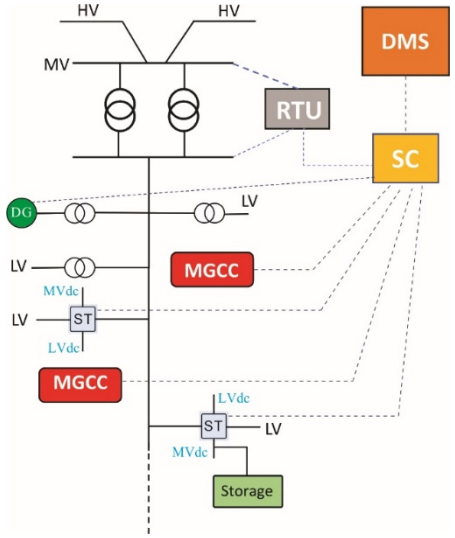

Fig. 15. MMG concept incorporating the ST.

By changing the ideal value of the frequency for the LV grid as function of the MV frequency, it is possible to induce the participation of the DERs located at the LV side in the power-frequency control strategy for the MMG. This modulation of the LV frequency is enabled whenever the MV frequency gets out of the dead-band (for example in the range of [49.8 50.2] Hz). As described previously, as soon as the MV frequency is within the dead band, the LV frequency cannot reach the nominal frequency as a result of the centralized secondary frequency control. Thus, a local integral controller (secondary frequency control) is included in order to eliminate the frequency deviation in the MG fed by a ST.

2) Primary and Secondary Frequency Control for Multi-Microgrid Autonomous Operation:

In the envisioned frame work for the autonomous operation of the MMG, the ST equipped with ESS will be the key enabler for the islanding operation, since their grid-inverters operate as GFM. Furthermore, to support the frequency control, other DERs located at the MV and LV grids are also able to participate in the primary control level. For that purpose, the distributed generation and the distributed energy storage are equipped with P-f droop characteristics in order to adapt the active power response according to the frequency deviation. The secondary frequency control is based on the computation of new set-points for the DERs connected to the MMG, aiming to bring the frequency to the nominal value (50 Hz). The set-points are defined by participation factors considering the reserve capacity provided by assets connected to the MV grid and by each MG. This control is supported by a communication infrastructure, which allows bidirectional communication between the control levels of the hierarchical architecture.

3) Multi-Microgrid Application-Examples: To exemplify the feasibility of the islanding operation for a MMG with ST, it was used a 15 kV MV feeder connected to the HV grid (60kV) through a HV/MV transformer. For simulation purpose, it was considered that in secondary substations 1, 4 and 8 STs have been installed. SS 1 has ESS operating as a GFM unit for both sides LV and MV. This MV feeder has also a small power

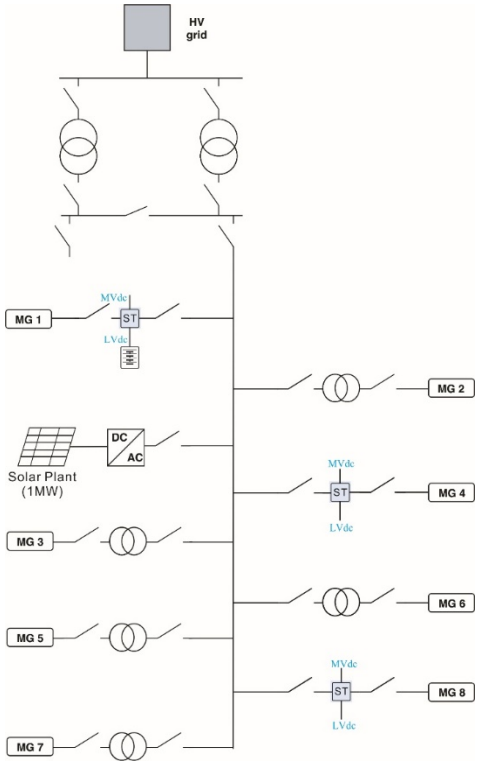

Fig. 16. MMG test system.

plant with an installed capacity around 1 MW, as described in Fig. 16.

Fig. 17 presents the simulations results for a scenario in which the MMG is exporting power to the HV grid prior to the islanding transient. When an intentional islanding occurs the MV frequency increases and the DERs connected to the MMG with P-f droop characteristics change their active power as response to the frequency variation. At t=18s, the centralized secondary frequency control is enabled, and from then on, the MV inverter is continuously reduced until to be zero. This means that from the MV side the grid is balanced (generation matches the load) by the definition of the set-points performed by the substation controller (SC). The droop characteristic LV frequency/MV frequency allows to transpose the MV frequency variations for the LV side to promote the participation of the local DERs in the global frequency control, as one can see in the moments subsequent to the disconnection from the upstream grid.

Although the MV frequency is stabilized in 50Hz, the simultaneous actuation of the centralized secondary frequency control and droop characteristic LV Angular frequency-MV

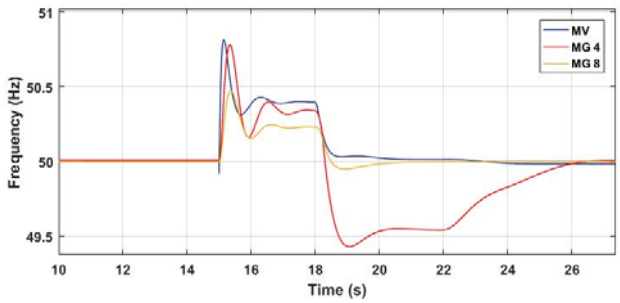

Fig. 17. MV, MG 4 and MG 8 frequencies during the transition to the islanded mode.

frequency lead to the frequency in the MG 4 and MG 8 to be different from the nominal value. When the centralized control stops its intervention, at the ST level, the local secondary frequency control is activated to conduct the LV frequency to the nominal value (t=22s).

D. Support to blackstart in active distribution grids

The presence of ST within the MMG, provides an environment where the control strategies described previously for the islanding operation can be adapted and extended to launch black start (BS) procedures.

When a blackout at the upstream voltage level or a fault in the HV grid occurs, an automatic transition to the islanding mode may not be successful. In this case, the DERs connected to the MMG associated with the ST inverters are coordinated to launch a service restoration procedure. The ST will then play an important role, especially if equipped with ESS once their grid inverters will operate as GFM units creating references for frequency and voltage within the MMG.

Besides, the service restoration procedure will be supported by a hierarchical control architecture and communication infrastructure. For this purpose a head controller of the MMG-the SC installed the HV/MV substation-will manage the BS procedures in accordance with a set of rules stored in its database. The SC will launch the BS procedure aiming to recover the system for pre-fault conditions (load levels, generation and distributed storage injection). After checking with Distribution Management System (DMS) that it is impossible to restore the service through the upstream grid, the SC will start a BS procedure following a top-down approach, characterized by sequence of actions:

1. Disconnect MV/LV transformers, DG units, distributed energy storage (DES) units, microgenerators and loads after the general blackout.

2. Sectionalizing the MMG around each ST with BS capability (equipped with ESS) to verify its capability to launch a local black start procedure.

3. Building MV/LV islands following a step-by-step process to avoid large inrush currents: The ST with BS capability will energize the MV lines and MV/LV electromagnetic transformers.

4. Soft start of the STs without storage trough the MV side, for example [21].

5. Disabling the local secondary frequency control in the ST without storage to allow the LV DERs participating in the power-frequency control.

6. Connecting of the DES with a pre-defined initial set-point (P=0) for supporting power-frequency control.

7. Connection of loads and distributed generation through the interaction among the three control layers: SC, Microgrid Central Controller (MGCC) and local controllers.

8. Enabling the centralized secondary frequency control based on the computation of participation factors for each MG and MV generation unit.

9. Activating the local secondary frequency control in the MG fed by a ST bringing the LV frequency to the nominal value.

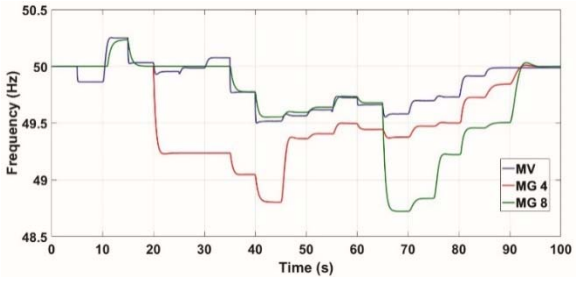

Fig. 18. MV, MG 4 and MG 8 frequencies during BS procedure.

10. Re-synchronization to the HV grid.

For the MV feeder presented in Fig. 17, a BS procedure as described previously was simulated. Fig. 18 describes the time evolution of the grid frequencies (MV, MG 4 an MG8) inside the MMG during the service restoration procedure. Those time evolutions reflect the behaviour of the control systems through the connection of loads and generation units. In this approach, neither the fast dynamics associated with the inrush currents resulting from the magnetization of the electromagnetic transformers nor the phenomena associated with the soft start-up of the ST are addressed.

After the connection of loads and generation is finished, at t=85, the SC sends a new set-point to the solar plant to inject the remaining active power (100 kW). From the figure, it is possible to observe that the frequencies are not in the nominal value (50Hz) at t=85s. Then, the centralised local secondary frequency control is activated and, consequently, MV frequency comes back to the nominal value (50 Hz) while the frequencies keep a deviation in MG 4 and MG 8. Those frequency deviations in MG 4 and MG 8 are afterwards eliminated. The top-down approach described previously assumes that the existing MGs do not have BS capability. Nevertheless, some secondary substations fed by electromagnetic transformers can be equipped with ESS. ESS connected to the LV busbar can operate as GFM unit for the LV grid. This allows islanding operation when it is not possible to keep the service through the MV level. In those cases, the MGCC can manage a parallel BS inside this MG, independently of the conditions in the MV grid. As further development of this top-down approach, one can design a combined BS strategy: a top-down process supported at the MV level by the ST and a local restoration procedure performed in MGs with BS capability. For those purposes, proper coordination strategies should be adopted for ensuring the synchronization of the LV grids to the MV grid. An important issue for designing the coordination strategies is to define the conditions for the synchronization. Still, the combined strategy will also be supported by the hierarchical control and communication infrastructure described.

V. Conclusions

In this paper, the smart transformer architecture and the provided advanced services, which improves the grid performances of the ac, dc and hybrid grid operating in radial and meshed networks-fed by smart transformer. The smart transformer can be controlled in either grid-forming or in grid-following mode, in which the smart transformer can be equivalent to a slack bus or PQ bus.

The ST will play an important role in the future distribution grids by providing significant operation flexibility improvements to the grid. It will enable the interconnection between AC and DC distribution grids, allowing the exploitation of meshed distribution networks where power flows can be con-trolled, and a more efficient direct integration of distributed DC resources such as PV power plants and electric vehicle DC charging stations. The ST's power converters can also be exploited to improve power quality in the AC grid sides by mitigating the harmonic distortion resulting from non-linear loads and DG units based on power converters, a phenomena expected to worsen in the coming years.

Apart from these features, the presence of ST serving as interface between MV and LV AC grids will enable other key functionalities when energy storage capacity is made available at ST's DC link, such as frequency and voltage control in the these grids, islanded operation and black-start supported by the ST's electronic power converters. Distribution System Operators need to look further to the potential of this new device as a mean to improve controllability of active distribution grids within the framework of the usage of new control and efficient management strategies to be adopted in the coming years.

VI. Refernces

[1] J. H. R. Enslin and P. J. M. Heskes, "Harmonic interaction between a large number of distributed power inverters and the distribution network," *IEEE Trans. Power Electron*., vol.19, no.6, pp.1586–1593, 2004.

[2] F. Wang, J. L. Duarte, M. A. M. Hendrix, and P. F. Ribeiro, "Modeling and analysis of grid harmonic distortion impact of aggregated dg inverters," *IEEE Transa. Power Electron*. vol.26, no.3, pp.786–797, 2011.

[3] M. Liserre, G. Buticchi, M. Andresen, G. De Carne, L. F. Costa, and Z. Zou, "The smart transformer: Impact on the electric grid and technology challenges," *IEEE Ind. Electron. Mag*., vol. 10, no. 2, pp. 46–58, 2016.

[4] J. Liu, J. Tang, F. Ponci, A. Monti, C. Muscas, and P. A. Pegoraro, "Trade-offs in PMU deployment for state estimation in active distribution grids," *IEEE Trans. Smart Grid*, vol.3, no.2, pp.915–924, 2012.

[5] G. Valverde and T. Van Cutsem, "Model predictive control of voltages in active distribution networks," *IEEE Trans. Smart Grid*, vol.4, no.4, pp.2152–2161, 2013.

[6] L. Ferreira Costa, G. De Carne, G. Buticchi, and M. Liserre, "The smart transformer: A solid-state transformer tailored to provide ancillary services to the distribution grid," *IEEE Power Electron. Mag*.,vol.4, no.2, pp.56–67, 2017.

[7] X. Gao, F. Sossan, K. Christakou, M. Paolone, and M. Liserre, "Con-current voltage control and dispatch of active distribution networks by means of smart transformer and storage," *IEEE Trans. Ind. Electron*., vol.65, no.8, pp.6657–6666, 2018.

[8] M. Liserre, M. Langwasser, R. Zhu, and C. Kumar, "Operation and control of smart transformer in meshed and hybrid grids," *IEEE Ind. Electron. Mag*., pp. 1–1, 2020, To be published.

[9] J. Rodrigues, C. Moreira, and J. P. Lopes, "Smart transformers as active interfaces enabling the provision of power-frequency regulation services from distributed resources in hybrid ac/dc grids," *Applied Sciences*, vol. 10, no. 4, 2020.

[10] Z. Zou, G. Buticchi, and M. Liserre, "Analysis and stabilization of a smart transformer-fed grid," *IEEE Trans. Ind. Electron*., vol. 65, no. 2, pp. 1325–1335, 2018.

[11] R. Zhu, Z. Zou, and M. Liserre, "High power quality voltage control of smart transformer-fed distribution grid," in IECON 2018 - 44th Annual

Conference of the IEEE Industrial Electronics Society, 2018, pp. 5547–5552.

[12] J. E. Huber and J. W. Kolar, "Solid-state transformers: On the origins and evolution of key concepts," *IEEE Ind. Electron. Mag.*, vol. 10, no. 3, pp. 19–28, 2016.

[13] F. Ruiz, M. A. Perez, J. R. Espinosa, T. Gajowik, S. Stynski, and M. Malinowski, "Surveying solid-state transformer structures and controls: Providing highly efficient and controllable power flow in distribution grids," *IEEE Ind. Electron. Mag.*, vol. 14, no. 1, pp. 56–70, 2020.

[14] H. Chen and D. Divan, "Soft-switching solid-state transformer (s4t)," *IEEE Trans. Power Electron.*, vol. 33, no. 4, pp. 2933–2947, 2018.

[15] D. Das, H. V M, C. Kumar, and M. Liserre, "Smart transformer enabled meshed hybrid distribution grid," *IEEE Trans. Ind. Electron.*, pp. 1–1, 2020, Early Access.

[16] J. Kuprat, M. Andresen, V. Raveendran, and M. Liserre, "Modular smart transformer topology for the interconnection of multiple isolated ac and dc grids," *2020 IEEE Energy Conversion Congress and Exposition (ECCE)*, Detroit, MI, USA, 2020, pp. 4836-4841.

[17] C. Kumar, X. Gao, and M. Liserre, "Smart transformer based loop power controller in radial power distribution grid," *in Proc. of 2018 IEEE PES Innovative Smart Grid Technologies Conference Europe (ISGT-Europe)*, 2018, pp. 1–6.

[18] R. Zhu, G. De Carne, F. Deng, and M. Liserre, "Integration of large photovoltaic and wind system by means of smart transformer," *IEEE Trans. Ind. Electron.*, vol. 64, no. 11, pp. 8928–8938, 2017.

[19] R. Zhu, Z. Zou, and M. Liserre, "High power quality voltage control of smart transformer-fed distribution grid," *in Proc. of IECON 2018 - 44th Annual Conference of the IEEE Industrial Electronics Society*, 2018, pp. 5547–5552.

[20] M. Couto, J. P. Lopes, and C. Moreira, "Control strategies for multi-microgrids islanding operation through smart transformers," *Electric Power Systems Research*, vol. 174, pp. 105-866, 2019.

[21] S. Pugliese, G. Buticchi, R. A. Mastromauro, M. Andresen, M. Liserre, and S. Stasi, "Soft-start procedure for a three-stage smart transformer based on dual-active bridge and cascaded H-bridge converters," *IEEE Trans. Power Electron.*, vol. 35, no. 10, pp. 11039–11052, 2020.

Rongwu Zhu (S'12-M'15) received the B.Eng. in Electrical Engineering from Nanjing Normal University, Nanjing, China, in 2007 and Ph.D. degree in energy technology from Department of Energy Technology, Aalborg University, Aalborg, Denmark, in 2015. From 2011-2012, he was a guest researcher with Aalborg University. He is currently a Senior Research with Chair of power electronics, at Christian-Albrechts-University of Kiel (Germany), and a full professor at the Harbin Institute of Technology (shenzhen), China.

He has authored and co-authored around 100 technical papers (over 1/3 of them in international peer-reviewed journals/magazine), and 6 patents. His research interests include renewable power generation system, operation and control of electric grid with high penetration of renewables, reliability and resilience improvement of power electronics dominated grid.

He served as a Guest Associate Editor of the IEEE Journal of Emerging and Selected Topics in Power Electronics, Guest Editor-in-Chief of the CSEE Journal of Power and Energy Systems, Editor of the International Transactions on Electrical Energy System, and Technical Committee Chair or Member of several international conferences.

Markus Andresen (S'5-M'7) received the M. Sc. degree in electrical engineering and business administration in 2012 and the Ph.D degree in 2017 from the chair of power electronics at Christian-Albrechts-Unversity of Kiel, Germany. In 2010, he was an intern in the Delta Shanghai Design Center at Delta Electronics (Shanghai) Co., Ltd., China and in 2017 he was a visiting scholar at the University of Wisconsin-Madison, USA. His current research interests include control of power converters and reliability in power electronics. Dr. Andresen was receipt of one IEEE price paper award on active thermal control of power electronics.

Marius Langwasser (S'16) received the B.Sc. and M.Sc. degree in electrical engineering and business administration at Kiel University, Kiel (Germany) in 2014 and 2016, respectively. Since 2016 he is scientific staff member and PhD student at the Chair of Power Electronics at Kiel University. Currently, he is responsible for the Kopernikus-project ENSURE and leading the group of hybrid grids. His research current interests include control and protection of hybrid grids and ancillary service provision with HVDC and Smart Transformers.

Marco Liserre (S'00-M'02-SM'07-F´13) received the MSc and PhD degree in Electrical Engineering from the Bari Polytechnic, respectively in 1998 and 2002. He has been Associate Professor at Bari Polytechnic and from 2012 Professor in reliable power electronics at Aalborg University (Denmark). From 2013 he is Full Professor and he holds the Chair of Power Electronics at Kiel University (Germany). He has published 500 technical papers (1/3 of them in international peer-reviewed journals) and a book. These works have received more than 35000 citations. Marco Liserre is listed in ISI Thomson report "The world's most influential scientific minds" from 2014.

He has been awarded with an ERC Consolidator Grant for the project "The Highly Efficient and Reliable smart Transformer (HEART), a new Heart for the Electric Distribution System".

He is member of IAS, PELS, PES and IES. He has been serving all these societies in different capacities. He has received the IES 2009 Early Career Award, the IES 2011 Anthony J. Hornfeck Service Award, the 2014 Dr. Bimal Bose Energy Systems Award, the 2011 Industrial Electronics Magazine best paper award and the Third Prize paper award by the Industrial Power Converter Committee at ECCE 2012, 2012, 2017 IEEE PELS Sustainable Energy Systems Technical Achievement Award and the 2018 IEEE-IES Mittelmann Achievement Award.

João A. Peças Lopes (S'80-M'94-F'16) is Full Professor at Porto University (FEUP) where he teaches in the graduation and post graduation areas. He is presently Associate Diretor and Coordinator of the TEC4Energy initiave at INESC TEC, one of the largest R&D interface institutions of the University of Porto. His main domains of research are related with large scale integration of renewable power sources, power system dynamics, microgeneration and microgrids, smart metering and electric vehicle grid integration.

He was Chair of the Selection Committee of the public tender that decided on the integration of 1800 MW of wind generation in Portugal, launched by the Portuguese government in 2005. He supervised 28 PhD Thesis. He is author or co-author of more than 400 papers and co-editor and co-author of the book "Electric Vehicle Integration into Modern Power Networks" edited by Springer. He has more than 9.000 citations in Scopus with an h index 43. He is a Fellow from IEEE. He is also member of the Power Systems Dynamic Performance Committee of the IEEE PES. He is Editor of the (SEGAN) Sustainable Energy Grids and Networks journal.

Carlos Moreira graduated in Electrical Engineering in the Faculty of Engineering of the University of Porto - FEUP (2003) and completed his PhD in Power Systems in November 2008, also from the University of Porto. He is a Senior Researcher in the Centre for Power and Energy Systems of INESC TEC since September 2003. In February 2009 he joined the Department of Electrical Engineering of FEUP as Assistant Professor. He lectures several classes in graduation and MSc courses in Electrical Engineering and Power Systems and supervises the research activities of several MSc and PhD students. His main research interests are related to microgrids operation and control, dynamics and stability analysis of electric power systems with increasing shares of converter interfaced generation systems and grid code development.

Justino Rodrigues has a Master degree in Electrical and Computer Engineering and is a researcher at INESC TEC in the Centre for Power Energy Systems. He is currently pursuing his PhD focused on exploring the "Smart-Transformer" concept for the development of AD/DC hybrid distribution networks and integration of distributed energy resources.

Mário Couto holds a master's degree in Electrical Engineering and Computers from the Faculty of Engineering of the University of Porto - FEUP (2010). He is part of the European Projects and Policies department of EDP Distribuição (main Portuguese DSO), managing the participation of the company in several European Projects funded by the European Commission. He started his professional career at INESC TEC, working on projects of loss reduction in electric distribution grids and in European projects about Smart Cities. In 2013 he moved for the EDP Distribuição, working for six years in the Medium Voltage Dispatch Centre. Currently, he is also developing his PhD studies on sustainable energy systems at the University of Porto.